

Active-Sterile neutrino masses and mixings in A_4 minimal extended seesaw mechanism

M. Kishan Singh^{1*}, S. Robertson^{1†}, N. Nimai Singh^{1,2‡}

¹Department of Physics, Manipur University, Imphal-795003, India.

²Research Institute of Science and Technology, Imphal-795003, India.

Abstract

Assuming the existence of an eV or KeV scale sterile neutrino, we develop a 3+1 neutrino mass model using $A_4 \times Z_4 \times Z_2$ symmetry group. Three Higgs H, H' and H'' are considered to give a desired neutrino mass matrix which generates non-zero θ_{13} . The model can give neutrino mixing parameters that are well within the experimental 3σ bounds. We also calculate the 4×4 active-sterile neutrino mixing matrix, and it is found to be consistent with experimental bounds.

Keywords– Sterile neutrino, Neutrino mixing, A_4 models, Active neutrinos, Beyond Standard model

*kishan@manipuruniv.ac.in

†robsoram@gmail.com

‡nimai03@yahoo.com

1 Introduction

The theory of neutrino masses and mixings has been a very highly exciting field of research in recent years. Observations from SNO, T2K, etc., that neutrinos have masses and oscillate among different flavors, have triggered a new approach in the study of neutrinos beyond the standard model (SM) framework. The three generations of leptonic mass squared differences and mixing angles have reached the precision measurement status. However, other parameters such as mass hierarchy, absolute neutrino mass, Dirac CP-violating phase are still unknown. The current global fit data for three neutrino oscillations [1] are shown in Table 1.

Apart from these, one interesting anomaly came from the experimental data of LSND [2], which observed excess of electron anti-neutrino ($\bar{\nu}_e$) in a muon anti-neutrino ($\bar{\nu}_\mu$) beam produced at the Los Alamos laboratory. Another experiment called, MiniBooNE [3] supplemented LSND results and observed an oscillation $\bar{\nu}_\mu$ to $\bar{\nu}_e$ compatible with the LSND data. These results can be interpreted by including more mass eigenstates of neutrino in the three neutrino theory [4]. One of the simplest ways is to add a fourth neutrino state, generally called the sterile neutrino, to the three active neutrinos [5]. The word sterile refers to the fact that such a neutrino can not have weak interactions in the SM from the requirement of being in agreement with the precision measurement of Z boson decay width at the LEP experiment. However, they can mix with the active neutrinos. It has been shown [6] in the 3+1 framework that the new analysis of the MiniBooNE data allows smaller values of active-sterile neutrino mixing for the standard analysis. Super-Kamiokande (SK) has provided upper bounds on sterile neutrino parameter $|U_{\tau 4}| < 0.18$ at 90% CL [7]. IceCube Collaborations [8] has also analyzed light sterile neutrinos from three years of atmospheric neutrino data from the DeepCore detector and provided limits on sterile neutrino mixing at $|U_{\mu 4}|^2 < 0.11$ and $|U_{\tau 4}|^2 < 0.15$ (90% C.L.) for the sterile neutrino mass splitting $\Delta m_{41}^2 = 1.0 \text{ eV}^2$. New data from the reactor and other short and long-baseline neutrino experiments such as MINOS [9], Daya Bay [10] etc., provide new bounds on active-sterile mixing and Δm_{41}^2 . Recently, it has been

parameter	best fit $\pm 1\sigma$	2σ range	3σ range
$ \Delta m_{21}^2 : [10^{-5}eV^2]$	$7.50^{+0.22}_{-0.20}$	7.11–7.93	6.94–8.14
$ \Delta m_{31}^2 : [10^{-3}eV^2](NO)$	$2.55^{+0.02}_{-0.03}$	2.49–2.60	2.47–2.63
$ \Delta m_{32}^2 : [10^{-3}eV^2](IO)$	$2.45^{+0.02}_{-0.03}$	2.39–2.50	2.37–2.53
$\sin^2 \theta_{12}/10^{-1}$	3.18 ± 0.16	2.86–3.52	2.71–3.69
$\sin^2 \theta_{23}/10^{-1}(NO)$	5.74 ± 0.14	5.41–5.99	4.34–6.10
$\sin^2 \theta_{23}/10^{-1}(IO)$	$5.78^{+0.10}_{-0.17}$	5.41–5.98	4.33–6.08
$\sin^2 \theta_{13}/10^{-2}(NO)$	$2.200^{+0.069}_{-0.062}$	2.069–2.337	2.000–2.405
$\sin^2 \theta_{13}/10^{-2}(IO)$	$2.225^{+0.064}_{-0.070}$	2.086–2.356	2.018–2.424
$\delta_{CP}/\pi(NO)$	$1.08^{+0.13}_{-0.12}$	0.84–1.42	0.71–1.99
$\delta_{CP}/\pi(IO)$	$1.58^{+0.15}_{-0.16}$	1.26–1.85	1.11–1.96

Table 1: Updated global-fit data for three neutrino oscillation [1].

reported from the MicroBooNE that there is no hint of an eV-scale sterile neutrino. But, GeV to KeV scale sterile neutrinos are still well-motivated theoretically and do not contradict any existing experiments. Besides, MicroBooNE does not probe the full parameter space of sterile neutrino models hinted at by MiniBooNE and other data, nor do they probe the ν_e interpretation of the MiniBooNE excess in a model-independent way [11]. Many other ongoing and future long-baseline experiments such as DUNE [12], T2HK [13], T2HKK [14] etc. may provide new insights on neutrino oscillation physics and explore active-sterile mixing. The phenomenology and experimental constraints on (3+1) neutrinos have been reviewed in [15–24].

Many authors have used discrete flavor symmetries of order n such as A_n , S_n , C_n , Z_n , etc., to develop models consistent with the current oscillation data. Several mechanisms have been used to study possible active-sterile mixing within the seesaw models. In Ref. [25], the authors have extensively studied minimal extended seesaw mechanism (MES) and their possible effects on cosmological problems such as baryogenesis, neutrinoless double beta decay, dark matter, etc. In the present work, we will use the MES mechanism

to explain active-sterile mixing. We use A_4 , Z_4 with three Higgs (one SM Higgs and two BSM Higgs) doublets with three A_4 triplet and three A_4 singlet flavon fields to explain possible active-sterile mixing in the normal hierarchy (NH). We take Z_2 symmetry group to remove unwanted interactions in the Lagrangian. We give different group charges to the fields resulting to new interactions and therefore, generate different neutrino mass matrix structures. We develop a (4×4) active-sterile neutrino mixing matrix from the model consistent with current experimental data. Moreover, there are searches for massive neutrinos, such as kinematic measurements of β -decay and searches for neutrinoless double beta decay ($0\nu\beta\beta$) events. The absolute neutrino mass scale is directly probed from the cut-off of the electron energy spectrum emitted from β -decay [26]. The effective neutrino mass m_β is given as

$$m_\beta = \left(\sum_{i=1}^4 |U_{ei}|^2 m_i^2 \right)^{1/2}, \quad (1)$$

where U is the 4×4 active-sterile neutrino mixing matrix. The effective mass parameter $m_{\beta\beta}$ from $0\nu\beta\beta$ can be expressed as the sum of mass eigenstates and mixing matrix elements as

$$m_{\beta\beta} = \left| \sum_{j=1}^4 U_{ej}^2 m_j \right|. \quad (2)$$

We solve these effective mass parameters from the model. The outline of this paper is as follows. We have a brief discussion about the MES mechanism in section 2, followed by the description of our model in section 3. In section 4, we will show the numerical analysis of the neutrino masses and mixing matrices and the results of our work. We will conclude with a summary and discussion in section 5.

2 Minimal extended seesaw mechanism

In this mechanism, along with the SM particles, we take three extra right-handed singlet neutrinos ($\nu_{R1}, \nu_{R2}, \nu_{R3}$) and one additional gauge singlet chi-

ral field S . It is possible to naturally generate an eV scale or KeV scale sterile neutrino mass with minimal but non-zero mixing with active neutrinos.

The general Lagrangian of neutrino mass terms is given by

$$-\mathcal{L} = \overline{\nu_L} M_D \nu_R + \frac{1}{2} \overline{\nu_R^c} M_R \nu_R + \overline{S^c} M_S \nu_R + h.c. \quad (3)$$

where M_D and M_R are the Dirac and Majorana mass matrices respectively. M_S is a (1×3) sterile neutrino mass matrix arising from the inclusion of only one extra singlet S . In the basis (ν_L, ν_R^c, S^c) , we get a full (7×7) matrix given by [5]

$$M_\nu^{7 \times 7} = \begin{pmatrix} 0 & M_D & 0 \\ M_D^T & M_R & M_S^T \\ 0 & M_S & 0 \end{pmatrix}. \quad (4)$$

In analogy to the canonical type-I seesaw, if we take the right-handed neutrino to be much higher than the electroweak scale of M_D , they should be decoupled at low scales. Therefore, we can block-diagonalise the (7×7) matrix by using the seesaw formula with the condition $M_R \gg M_D$ and get a (4×4) neutrino mass matrix in the basis (ν_L, S^c) as

$$M_\nu^{4 \times 4} = - \begin{pmatrix} M_D M_R^{-1} M_D^T & M_D M_R^{-1} M_S^T \\ M_S (M_R^{-1})^T M_D^T & M_S M_R^{-1} M_S^T \end{pmatrix}. \quad (5)$$

We have four light neutrino eigenstates corresponding to three active neutrinos and one sterile neutrino. As we can see in eq. (5), $\det(M_\nu^{4 \times 4}) = 0$. This means that at least one of the four light neutrinos is massless. We further proceed to diagonalize the above 4×4 mass matrix with the seesaw condition that $M_D < M_S$, we obtain a leading order of the active neutrino mass matrix m_ν as well as the sterile mass m_s given as follows.

$$m_\nu \simeq M_D M_R^{-1} M_S^T (M_S M_R^{-1} M_S^T)^{-1} M_S (M_R^{-1})^T M_D^T - M_D M_R^{-1} M_D^T; \quad (6)$$

$$m_s \simeq -M_S M_R^{-1} M_S^T. \quad (7)$$

We can naturally produce a sterile neutrino having mass in the eV scale. For example, if we take $M_D \sim 10^2$ GeV, $M_R \sim 5 \times 10^{14}$ GeV and $M_S \sim 5 \times 10^2$

GeV , we get approximately $m_\nu \sim 0.02$ eV and $m_s \sim 0.5$ eV. Further, as pointed out in Ref. [27], a slightly higher keV scale sterile neutrino can also be generated if we increase the M_S mass scale upto TeV scale, which is also possible in MES mechanism.

The 3×3 active neutrino mass matrix m_ν can be diagonalized by a unitary 3×3 complex matrix U_{PMNS} as [28]

$$m_\nu = U_{PMNS} \cdot \text{diag}(m_1, m_2, m_3) \cdot U_{PMNS}^T. \quad (8)$$

In MES scheme, for NH: ($m_1 \ll m_2 < m_3 \ll m_4$), the light neutrino masses including the eV or KeV mass scale sterile neutrino are given in terms of mass-squared differences as

$$m_1 = 0 ; \quad m_2 = \sqrt{\Delta m_{21}^2} ; \quad m_3 = \sqrt{\Delta m_{21}^2 + \Delta m_{31}^2} ; \quad m_4 = \sqrt{\Delta m_{41}^2},$$

where $\Delta m_{ij}^2 = |m_j^2 - m_i^2|$.

U_{PMNS} can be parameterized using three mixing angles $\theta_{12}, \theta_{13}, \theta_{23}$ and one CP violating phase δ_{13} for Dirac neutrinos and two Majorana phases α and β for Majorana neutrinos. In PDG convention, the general form of U_{PMNS} is

$$U_{PMNS} = \begin{pmatrix} 1 & 0 & 0 \\ 0 & c_{23} & s_{23} \\ 0 & -s_{23} & c_{23} \end{pmatrix} \begin{pmatrix} c_{13} & 0 & e^{-i\delta_{13}} s_{13} \\ 0 & 1 & 0 \\ -e^{-i\delta_{13}} s_{13} & 0 & c_{13} \end{pmatrix} \begin{pmatrix} c_{12} & s_{12} & 0 \\ -s_{12} & c_{12} & 0 \\ 0 & 0 & 1 \end{pmatrix} P, \quad (9)$$

where $c_{ij} = \cos \theta_{ij}$, $s_{ij} = \sin \theta_{ij}$ and $P = \text{diag}(1, e^{i\alpha}, e^{i(\beta+\delta_{13})})$ is the Majorana phase matrix.

In the 3+1 mixing framework, the leptonic mixing matrix U_{PMNS} is not strictly unitary due to contributions from the sterile sector. But, because of minimal active-sterile mixing, we can assume that U_{PMNS} is unitary at the $\mathcal{O}(10^{-2})$ level [29]. The full 4×4 neutrino mixing matrix takes the form [30]

$$V \simeq \begin{pmatrix} (1 - \frac{1}{2}RR^\dagger)U_{PMNS} & R \\ -R^\dagger U_{PMNS} & 1 - \frac{1}{2}R^\dagger R \end{pmatrix}, \quad (10)$$

where R is a 3×1 matrix which determines the strength of active-sterile mixing and

$$R = M_D M_R^{-1} M_S^T (M_S M_R^{-1} M_S^T)^{-1}. \quad (11)$$

Taking the same mass scales as shown above, we estimate $R \sim 0.2$ for m_s in eV scale and $R \sim 0.1$ for m_s in KeV scale, both of which are in good agreement with experimental data of active-sterile neutrino mixing.

The 4×4 neutrino mixing matrix can also be parameterized by six mixing angles $(\theta_{12}, \theta_{13}, \theta_{23}, \theta_{14}, \theta_{24}, \theta_{34})$, three Dirac phases $(\delta_{13}, \delta_{14}, \delta_{24})$ and three Majorana phases (α, β, γ) [18].

$$U^{4 \times 4} = \begin{pmatrix} c_{12}c_{13}c_{14} & c_{13}c_{14}s_{12}e^{i\frac{\alpha}{2}} & c_{14}s_{13}e^{i\frac{\beta}{2}} & s_{14}e^{-i\frac{\gamma}{2}} \\ U_{\mu 1} & U_{\mu 2} & U_{\mu 3} & c_{14}s_{24}e^{-i(\frac{\gamma}{2}-\delta_{14}+\delta_{24})} \\ U_{\tau 1} & U_{\tau 2} & U_{\tau 3} & c_{14}c_{24}s_{34}e^{-i(\frac{\gamma}{2}-\delta_{14})} \\ U_{s1} & U_{s2} & U_{s3} & c_{14}c_{24}c_{34}e^{-i(\frac{\gamma}{2}-\delta_{14})} \end{pmatrix}. \quad (12)$$

Comparing eq. (10) and eq. (12), we obtain the relation between neutrino mixing angles and the elements of mixing matrix as

$$\sin^2 \theta_{14} = |V_{e4}|^2 \quad (13)$$

$$\sin^2 \theta_{24} = \frac{|V_{e4}|^2}{1 - |V_{e4}|^2} \quad (14)$$

$$\sin^2 \theta_{34} = \frac{|V_{\tau 4}|^2}{1 - |V_{e4}|^2 - |V_{\mu 4}|^2} \quad (15)$$

$$\sin^2 \theta_{12} = \frac{|V_{e2}|^2}{1 - |V_{e4}|^2 - |V_{e3}|^2} \quad (16)$$

$$\sin^2 \theta_{13} = \frac{|V_{e3}|^2}{1 - |V_{e4}|^2} \quad (17)$$

$$\sin^2 \theta_{23} = \frac{|V_{e3}|^2(1 - |V_{e4}|^2) - |V_{e4}|^2|V_{\mu 4}|^2}{1 - |V_{e4}|^2 - |V_{\mu 4}|^2} \quad (18)$$

$$+ \frac{|V_{e1}V_{\mu 1} + V_{e2}V_{\mu 2}|^2(1 - |V_{e4}|^2)}{(1 - |V_{e4}|^2 - |V_{e3}|^2)(1 - |V_{e4}|^2 - |V_{\mu 4}|^2)} \quad (19)$$

$$(20)$$

where V_{ij} are the elements of mixing matrix (10).

$\frac{Fields}{Charges}$	l	e_R	μ_R	τ_R	H	H'	H''	ϕ	ψ	χ	χ'	ζ	ν_{R1}	ν_{R2}	ν_{R3}	S
$SU(2)_L$	2	1	1	1	2	2	2	1	1	1	1	1	1	1	1	1
A_4	3	1	1''	1'	1'	1	1	3	3	1	1'	1	1'	1	1'	1''
Z_4	1	1	1	1	1	-i	i	-i	1	1	1	-1	i	-1	1	-i
Z_2	1	1	1	1	1	-1	1	1	1	1	1	1	1	-1	1	1

Table 2: Particle contents of the model and their group charges.

3 Model Description

This model uses the A_4 discrete group to develop the neutrino mass matrices along with Z_4 and Z_2 in normal hierarchy (NH) only. A_4 has four irreducible representations in which three are singlets ($1, 1', 1''$) and one is triplet(3) [31]. We take the SM charged lepton doublet l as triplet under A_4 and the right-handed charged lepton singlets (e_R, μ_R, τ_R) as singlets ($1, 1'', 1'$) respectively. It is convenient to extend the SM Higgs H by adding two more BSM Higgs H' and H'' which are singlets under A_4 to produce a mass model consistent with the current experimental data. We use two A_4 triplet flavons ϕ and ψ for generating M_L and M_D and two singlets (χ, χ') which will give the Majorana mass matrix. Another singlet flavon ζ is responsible for generating the sterile mass matrix M_S . The full particle contents and their group charges are shown in Table 2. The invariant Lagrangian for the leptonic interactions is given by

$$\mathcal{L} = \mathcal{L}_{M_L} + \mathcal{L}_{M_D} + \mathcal{L}_{M_R} + \mathcal{L}_{M_S} + h.c. \quad (21)$$

where,

$$\mathcal{L}_{M_L} = \frac{y_e}{\Lambda} (\bar{l} H \psi)_{1e_R} + \frac{y_\mu}{\Lambda} (\bar{l} H \psi)_{1'\mu_R} + \frac{y_\tau}{\Lambda} (\bar{l} H \psi)_{1''\tau_R} \quad (22)$$

$$\mathcal{L}_{M_D} = \frac{y_1}{\Lambda} (\bar{l} \tilde{H} \phi)_{1''\nu_{R1}} + \frac{y_2}{\Lambda} (\bar{l} \tilde{H}' \phi)_{1\nu_{R2}} + \frac{y_3}{\Lambda} (\bar{l} \tilde{H} \psi)_{1''\nu_{R3}} \quad (23)$$

$$\mathcal{L}_{M_R} = \frac{1}{2} \lambda_1 \chi' \bar{\nu}_{R1}^c \nu_{R1} + \frac{1}{2} \lambda_2 \chi \bar{\nu}_{R2}^c \nu_{R2} + \frac{1}{2} \lambda_3 \chi' \bar{\nu}_{R3}^c \nu_{R3} \quad (24)$$

$$\mathcal{L}_{M_S} = \frac{1}{2} k \zeta \bar{S}^c \nu_{R1} \quad (25)$$

The constant Λ denotes the cut-off scale and $\tilde{H} = i\tau_2 H$ (where τ_2 is the second Pauli matrix) is used in order to make the Lagrangian gauge invariant

whereas y_i, y_j, λ_j, k where $i = e, \mu, \tau; j = 1, 2, 3$ respectively, are the Yukawa coupling constants. Z_2 is used to remove the term $\frac{y_1}{\Lambda}(\bar{l}\tilde{H}'\psi)_{1''}\nu_{R1}$ from \mathcal{L}_{M_D} . If we choose the T -diagonal basis of A_4 along with the flavon vev alignments [22]

$$\langle\phi\rangle = (v, 0, 0) \quad ; \quad \langle\psi\rangle = (v, v, v) \quad ; \quad \langle\chi\rangle = \langle\chi'\rangle = v \quad ; \quad \langle\zeta\rangle = u. \quad (26)$$

then, we get a diagonal charged lepton mass matrix

$$M_L = \frac{\langle H \rangle v}{\Lambda} \text{diag}(y_e, y_\mu, y_\tau) \quad (27)$$

The Dirac, Majorana and sterile mass matrices takes the following forms

$$M_D^o = \frac{\langle H \rangle v}{\Lambda} \begin{pmatrix} y_1 & y_2 & 0 \\ y_1 & y_2 & 0 \\ y_1 & y_2 & y_3 \end{pmatrix} = \begin{pmatrix} a & b & 0 \\ a & b & 0 \\ a & b & c \end{pmatrix}; \quad (28)$$

$$M_R = v \begin{pmatrix} \lambda_1 & 0 & 0 \\ 0 & \lambda_2 & 0 \\ 0 & 0 & \lambda_3 \end{pmatrix} = \begin{pmatrix} d & 0 & 0 \\ 0 & e & 0 \\ 0 & 0 & f \end{pmatrix}; \quad (29)$$

$$M_S = \begin{pmatrix} ku & 0 & 0 \end{pmatrix}, \quad (30)$$

where $a = \frac{\langle H \rangle v}{\Lambda} y_1, b = \frac{\langle H \rangle v}{\Lambda} y_2, c = \frac{\langle H \rangle v}{\Lambda} y_3, d = \lambda_1 v, e = \lambda_2 v, f = \lambda_3 v$.

Applying MES mechanism with these mass matrices in eq. (6), we obtain the active neutrino mass matrix as

$$m_\nu^o = - \begin{pmatrix} \frac{b^2}{e} & \frac{b^2}{e} & \frac{b^2}{e} \\ \frac{b^2}{e} & \frac{b^2}{e} & \frac{b^2}{e} \\ \frac{b^2}{e} & \frac{b^2}{e} & \frac{b^2}{e} + \frac{c^2}{f} \end{pmatrix}. \quad (31)$$

It is easy to see that m_ν^o is a $\mu - \tau$ symmetric matrix which give $\theta_{13} = 0$.

But, recent experimental data has proven θ_{13} to be non-zero. In order to generate $\theta_{13} \neq 0$, M_D^o is modified by adding a perturbation term M'_D . We can achieve this if we introduce an $SU(2)_L$ singlet flavon η having $A_4 \otimes Z_4 \otimes Z_2$ charges $(3, -i, 1)$ with vev alignment of $(0, 0, v)$ in our model. The Lagrangian responsible for the perturbation matrix is

$$\mathcal{L}_{M'_D} = \frac{y_4}{\Lambda} (\bar{l}\eta)_{1'} \tilde{H} \nu_{R1} + \frac{y_4}{\Lambda} (\bar{l}\eta)_1 \tilde{H}' \nu_{R2} + \frac{y_4}{\Lambda} (\bar{l}\eta)_{1''} \tilde{H}'' \nu_{R3} \quad (32)$$

Then, the perturbation matrix looks like

$$M'_D = \frac{\langle H \rangle v}{\Lambda} \begin{pmatrix} 0 & 0 & y_4 \\ 0 & y_4 & 0 \\ y_4 & 0 & 0 \end{pmatrix}. \quad (33)$$

The resultant active neutrino mass matrix with $M_D = M_D^o + M'_D$ from eq. (6) becomes

$$m_\nu \simeq - \begin{pmatrix} \frac{b^2}{e} + \frac{t^2}{f} & \frac{b(b+t)}{e} & \frac{b^2}{e} + \frac{ct}{f} \\ \frac{b(b+t)}{e} & \frac{(b+t)^2}{e} & \frac{b(b+t)}{e} \\ \frac{b^2}{e} + \frac{ct}{f} & \frac{b(b+t)}{e} & \frac{b^2}{e} + \frac{c^2}{f} \end{pmatrix}, \quad (34)$$

where $t = \frac{\langle H \rangle v}{\Lambda} y_4$, and y_4 is the Yukawa coupling for the perturbation term.

The sterile neutrino mass is obtained from eq. (7) as

$$m_s \simeq - \left(\frac{g^2}{d} \right), \quad (35)$$

where $g = ku$.

The numerical bounds of the model parameters and mixing parameters obtained from our model will be determined in the next section through numerical analysis.

4 Numerical Analysis and Results

To validate the present model, we first try to solve the free parameters by comparing the LHS and RHS of eq. (8). We take the current 3σ values of mixing angles, and mass squared differences from Table 1. We vary the unknown Majorana phases in the range $(0, 2\pi)$ and we have fixed non-degenerate values for the heavy right-handed neutrino mass parameters $d = e \simeq 10^{13}$ GeV and $f \simeq 5 \times 10^{13}$ GeV. We numerically solve the model parameters b, c and t which satisfy the five independent equations with a tolerance of $\mathcal{O}(10^{-2})$. The correlation plots among different models parameters are shown in Fig. 1. We find that the parameter space is very narrow, which can be verified or discarded in future experiments.

Remaining parameters a and g are solved using the 3σ bounds on active-sterile mass-squared difference $|\Delta m_{41}^2| \in (0.87, 2.04)$ eV² [32–34]. Now, the model-dependent 4×4 mixing matrix V can be developed in eq. (10) from which we can solve other mixing parameters using eq. (13) - eq. (20). The variation of different mixing angles with perturbation parameter t are shown in Fig. 2. It is observed that many data points of t are available within the 3σ ranges of the mixing angles. More data points are concentrated at regions $\sin^2 \theta_{23} > 0.50$ which implies that the model favours higher octant of θ_{23} . Fig. 3 shows the variation of active-sterile mixing elements. Allowed 3σ bounds are shown in the plots and it can be seen that the present model can give values within the experimental bounds.

Parameters	3σ range (GeV)	Best-fit (GeV)
$ b $	2.05 - 9.11	4.45
$ c $	32.11 - 40.35	35.70
$ t $	10.75 - 18.41	17.01
$ a $	9.56 - 21.03	14.68
$ g $	96.66 - 119.53	106.77

Table 3: 3σ range and the best-fit values of the model parameters.

In case where mixing variables in eq. (8) take best-fit values from Table 1 and taking Majorana phases to be zero for simplicity, we determine the model parameters and they are shown in Table 3. The resulting best-fit 4×4 mixing matrix is obtained as

$$U_{bf} = \begin{pmatrix} 0.7969 & 0.5584 & 0.1665 & 0.1375 \\ -0.2980 + 0.0211i & 0.6011 + 0.0154i & -0.7075 - 0.1811i & 0.1375 \\ 0.6788 + 0.0719i & -0.5711 + 0.0129i & -0.5858 - 0.1497i & 0.2968 \\ -0.2879 - 0.0282i & 0.0107 - 0.0040i & 0.2644 + 0.0755i & 0.9370 \end{pmatrix}$$

We can observe that the elements of the mixing matrix are well within the allowed ranges of oscillation data.

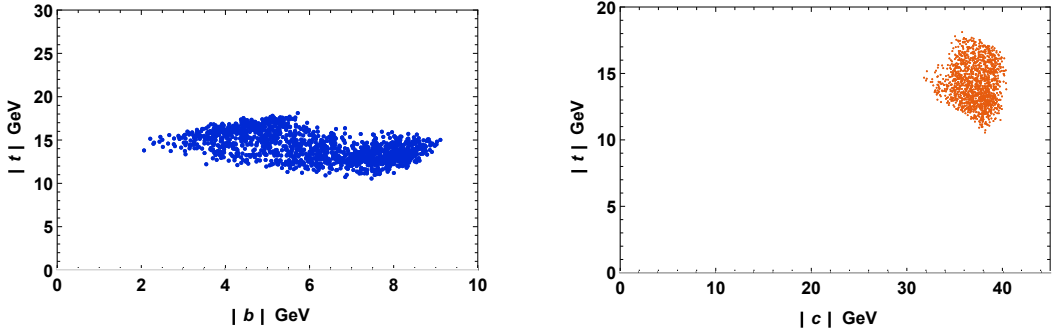


Figure 1: Variation of model parameters are shown as correlation plots with each other.

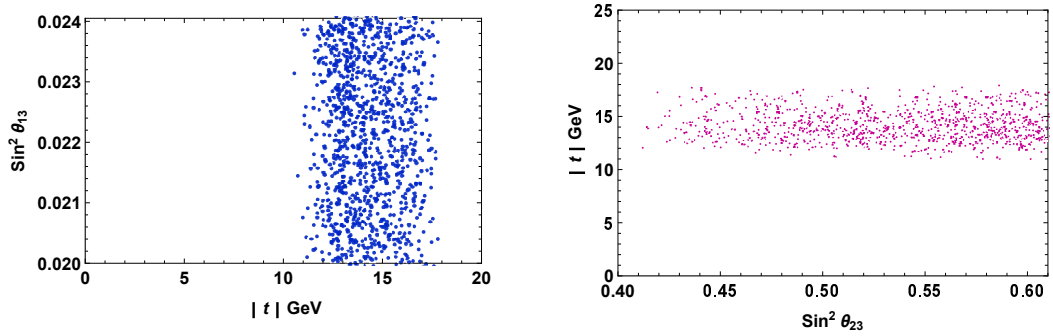


Figure 2: Variation of perturbation parameters t with mixing angles.

We also calculate the effective neutrino mass m_β and $m_{\beta\beta}$ and plot their variations in Fig. 4. We find that the mixing angles and effective neutrino mass parameters are within their allowed ranges.

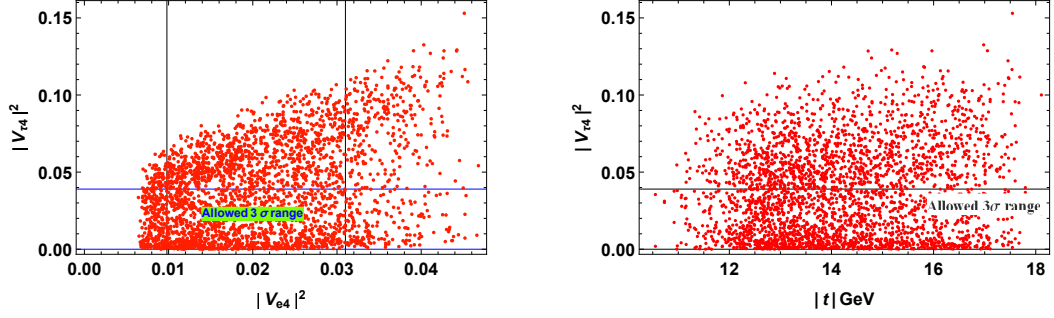


Figure 3: Variation of active-sterile mixing element $|V_{e4}|^2$ with $|V_{\tau 4}|^2$ and with model parameter t .

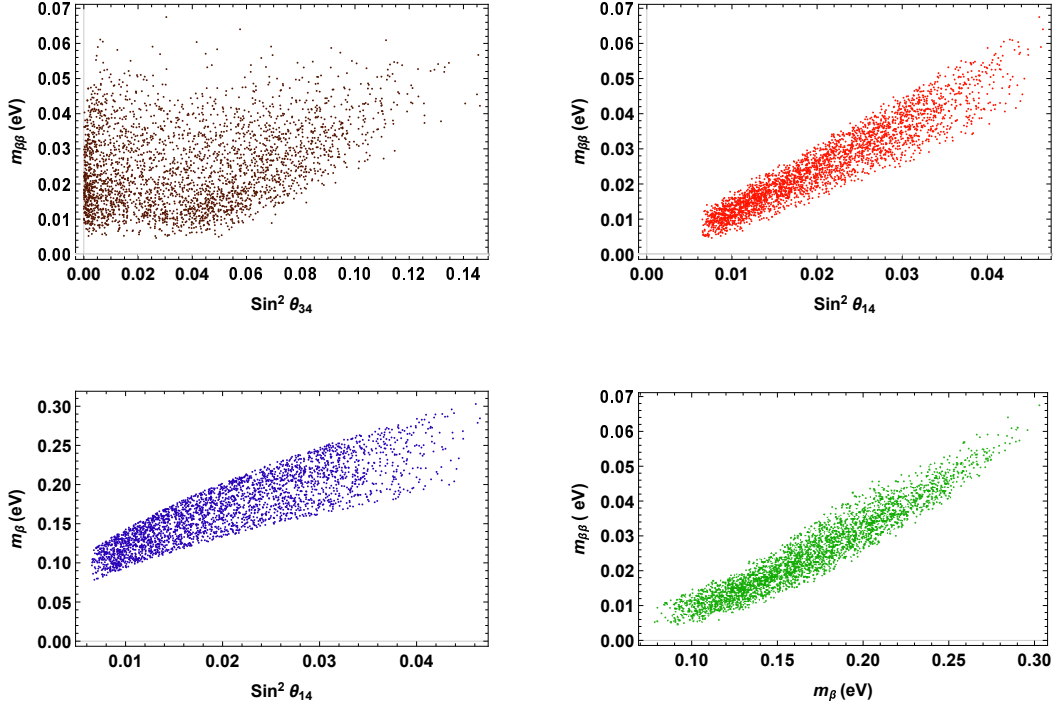


Figure 4: Variation of effective neutrino mass m_{β} and $m_{\beta\beta}$ with active-sterile mixing angles

5 Summary and discussion

In this work, we have developed an A_4 model supplemented by Z_4 and Z_2 groups. One singlet sterile neutrino is added to the 3-neutrino theory to explain 3 + 1 active sterile neutrino masses and mixings. Addition of triplet

flavon η gives the desired $\mu - \tau$ symmetry breaking active neutrino mass matrix. The active sterile mixing matrix R provides the non-unitary contribution to the active mixing matrix U_{PMNS} . By constraining the light neutrino masses m_1, m_2, m_3 and m_4 from the experimental mass-squared difference at 3σ , we have determined the parameters of the model. It is observed that the parameters lie in the low GeV scale, which can be verified in future experiments. We have plotted the bounds on the active sterile mixing $|V_{\mu 4}|^2$ and $|V_{\tau 4}|^2$ from our model by fixing $|\Delta m_{41}^2|$ and $|V_{e4}|^2$. A large number of data points are concentrated within the allowed ranges. We also calculate the effective mass parameters m_β and $m_{\beta\beta}$. Their values are obtained in the ranges $0.0784 \text{ eV} < m_\beta < 0.3034 \text{ eV}$ and $0.00342 \text{ eV} < m_{\beta\beta} < 0.06675 \text{ eV}$ respectively. This is allowed in the latest upper bound $m_\beta < 1.1 \text{ eV}$ at 90% confidence level recently published by the KATRIN Collaborations [35]. This is also in agreement with the results of the analysis in Ref. [26], where active neutrinos mixing with light sterile sterile neutrino leads to an upper limit of $m_\beta < 0.09 \text{ eV}$ and $m_{\beta\beta} < 0.07 \text{ eV}$ at 95% CL.

At current status, the bounds on active-sterile mass squared difference $|\Delta m_{41}|^2$ is still not known. Many experiments give various constraints, such as, $|\Delta m_{41}|^2 = 1.7\text{eV}^2$ [36], $|\Delta m_{41}|^2 = 4.5\text{eV}^2$ [37], $|\Delta m_{41}|^2 < 10\text{eV}^2$ [38], $|\Delta m_{41}|^2 = 7.3 \pm 1.17\text{eV}^2$ [39], etc. We have chosen a particular bound and performed the numerical analysis. We have also determined the best-fit 4×4 mixing matrix resulting from the model and found that the mixing parameters satisfy the current 3σ bounds of the mixing matrix. In conclusion, we can remark that we have developed a model framework which is possible to explain the origin of neutrino masses and mixings through discrete symmetry. It can also generate possible active-sterile mixing in the 3+1 MES mechanism.

Acknowledgements

We wish to thank Prof. M. K. Das of Tezpur University for giving us many fruitful suggestions in this work. One of us (MKS), would also like to thank DST-INSPIRE, Govt. of India, for providing financial support under DST-

INSPIRE Fellowship.

References

- [1] Ivan Esteban, M.C. Gonzalez-Garcia, Michele Maltoni, Thomas Schwetz, and Albert Zhou. The fate of hints: updated global analysis of three-flavor neutrino oscillations. *Journal of High Energy Physics*, 2020(9), Sep 2020.
- [2] A Aguilar-Arevalo, LSND collaboration, et al. Evidence for neutrino oscillations from the observation of anti-neutrino (electron) appearance in a anti-neutrino (muon) beam. *Phys. Rev. D*, 64:112007, 2001.
- [3] AA Aguilar-Arevalo, BC Brown, L Bugel, G Cheng, JM Conrad, RL Cooper, R Dharmapalan, A Diaz, Z Djurcic, DA Finley, et al. Significant excess of electronlike events in the mini-boone short-baseline neutrino experiment. *Physical review letters*, 121(22):221801, 2018.
- [4] Mona Dentler, Álvaro Hernández-Cabezudo, Joachim Kopp, Pedro A. N. Machado, Michele Maltoni, Ivan Martinez-Soler, and Thomas Schwetz. Updated Global Analysis of Neutrino Oscillations in the Presence of eV-Scale Sterile Neutrinos. *JHEP*, 08:010, 2018.
- [5] He Zhang. Light Sterile Neutrino in the Minimal Extended Seesaw. *Phys. Lett. B*, 714:262–266, 2012.
- [6] C Giunti, A Ioannisian, and G Ranucci. A new analysis of the mini-boone low-energy excess. *Journal of High Energy Physics*, 2020(11):1–14, 2020.
- [7] Ko Abe, Y Haga, Y Hayato, M Ikeda, K Iyogi, J Kameda, Y Kishimoto, M Miura, S Moriyama, M Nakahata, et al. Limits on sterile neutrino mixing using atmospheric neutrinos in super-kamiokande. *Physical Review D*, 91(5):052019, 2015.
- [8] MG Aartsen, M Ackermann, J Adams, JA Aguilar, M Ahlers, M Ahrens, I Al Samarai, D Altmann, K Andeen, T Anderson, et al. Search for ster-

- ile neutrino mixing using three years of icecube deepcore data. *Physical Review D*, 95(11):112002, 2017.
- [9] P Adamson, DJ Auty, DS Ayres, C Backhouse, G Barr, M Bishai, A Blake, GJ Bock, DJ Boehnlein, D Bogert, et al. Active to sterile neutrino mixing limits from neutral-current interactions in minos. *Physical review letters*, 107(1):011802, 2011.
 - [10] FP An, AB Balantekin, HR Band, W Beriguete, M Bishai, S Blyth, I Butorov, GF Cao, J Cao, YL Chan, et al. Search for a light sterile neutrino at daya bay. *Physical review letters*, 113(14):141802, 2014.
 - [11] CA Argüelles, I Esteban, M Hostert, KJ Kelly, J Kopp, PAN Machado, I Martinez-Soler, and YF Perez-Gonzalez. Microboone and the ν_e interpretation of the miniboone low-energy excess. *arXiv preprint arXiv:2111.10359*, 2021.
 - [12] R Acciarri, MA Acero, M Adamowski, C Adams, P Adamson, S Adhikari, Z Ahmad, CH Albright, T Alion, E Amador, et al. Long-baseline neutrino facility (lbnf) and deep underground neutrino experiment (dune) conceptual design report, volume 4 the dune detectors at lbnf. *arXiv preprint arXiv:1601.02984*, 2016.
 - [13] K Abe, T Abe, H Aihara, Y Fukuda, Y Hayato, K Huang, AK Ichikawa, M Ikeda, K Inoue, H Ishino, et al. Letter of intent: The hyper-kamiokande experiment—detector design and physics potential—. *arXiv preprint arXiv:1109.3262*, 2011.
 - [14] Hyper-Kamiokande proto Collaboration, Ke Abe, Ke Abe, SH Ahn, H Aihara, A Aimi, R Akutsu, C Andreopoulos, I Anghel, LHV Anthony, et al. Physics potentials with the second hyper-kamiokande detector in korea. *Progress of Theoretical and Experimental Physics*, 2018(6):063C01, 2018.
 - [15] Leonard S Kisslinger. Sterile plus active neutrinos and neutrino oscillations. *International Journal of Theoretical Physics*, 53(9):3201–3207, 2014.

- [16] S. Dev, Desh Raj, Radha Raman Gautam, and Lal Singh. New mixing schemes for $(3+1)$ neutrinos. *Nuclear Physics B*, 941:401–424, 2019.
- [17] James Barry, Werner Rodejohann, and He Zhang. Light sterile neutrinos: models and phenomenology. *Journal of High Energy Physics*, 2011(7):1–28, 2011.
- [18] Stefano Gariazzo, C Giunti, M Laveder, YF Li, and EM Zavanin. Light sterile neutrinos. *Journal of Physics G: Nuclear and Particle Physics*, 43(3):033001, 2016.
- [19] Yongchao Zhang, Xiangdong Ji, and Rabindra N Mohapatra. A naturally light sterile neutrino in an asymmetric dark matter model. *Journal of High Energy Physics*, 2013(10):1–19, 2013.
- [20] Yongchao Zhang. Majorana neutrino mass matrices with three texture zeros and the sterile neutrino. *Physical Review D*, 87(5):053020, 2013.
- [21] Debasish Borah. Nonzero θ_{13} with unbroken μ - τ symmetry of the active neutrino mass matrix in the presence of a light sterile neutrino. *Physical Review D*, 95(3):035016, 2017.
- [22] Pritam Das and Mrinal Kumar Das. keV Sterile Neutrino Mass Model and Related Phenomenology. *Springer Proc. Phys.*, 265:167–172, 2022.
- [23] Pritam Das, Ananya Mukherjee, and Mrinal Kumar Das. Active and Sterile Neutrino Phenomenology with A_4 -Based Minimal Extended Seesaw. *Springer Proc. Phys.*, 261:969–975, 2021.
- [24] Pritam Das, Mrinal Kumar Das, and Najimuddin Khan. Phenomenological study of neutrino mass, dark matter and baryogenesis within the framework of minimal extended seesaw. *JHEP*, 03:018, 2020.
- [25] Pritam Das. Theoretical and phenomenological consequences of active and sterile neutrino within Beyond Standard Model framework. Other thesis, 7 2021.

- [26] Steffen Hagstotz, Pablo F. de Salas, Stefano Gariazzo, Sergio Pastor, Martina Gerbino, Massimiliano Lattanzi, Sunny Vagnozzi, and Katherine Freese. Bounds on light sterile neutrino mass and mixing from cosmology and laboratory searches. *Physical Review D*, 104(12), 12 2021.
- [27] Basudeb Dasgupta and Joachim Kopp. Sterile neutrinos. *Physics Reports*, 928:1–63, Sep 2021.
- [28] Jose WF Valle. Neutrino physics overview. In *Journal of Physics: Conference Series*, volume 53, page 031. IOP Publishing, 2006.
- [29] Zhi zhong Xing. Flavor structures of charged fermions and massive neutrinos. *Physics Reports*, 854:1–147, apr 2020.
- [30] J Schechter and José WF Valle. Neutrino decay and spontaneous violation of lepton number. *Physical Review D*, 25(3):774, 1982.
- [31] Hajime Ishimori, Tatsuo Kobayashi, Hiroshi Ohki, Yusuke Shimizu, Hiroshi Okada, and Morimitsu Tanimoto. Non-Abelian Discrete Symmetries in Particle Physics. *Prog. Theor. Phys. Suppl.*, 183:1–163, 2010.
- [32] Max Aker, Konrad Altenmüller, Marius Arenz, Woo-Jeong Baek, John Barrett, Armen Beglarian, Jan Behrens, Anatoly Berlev, Uwe Besserer, Klaus Blaum, et al. First operation of the katrin experiment with tritium. *The European Physical Journal C*, 80(3):1–18, 2020.
- [33] Srubabati Goswami, Ananya Mukherjee, Nimmala Narendra, et al. Leptogenesis and $e\nu$ scale sterile neutrino. *arXiv preprint arXiv:2111.14719*, 2021.
- [34] Nabila Aghanim, Yashar Akrami, Mark Ashdown, J Aumont, C Baccigalupi, M Ballardini, AJ Banday, RB Barreiro, N Bartolo, S Basak, et al. Planck 2018 results-vi. cosmological parameters. *Astronomy & Astrophysics*, 641:A6, 2020.
- [35] Max Aker, K Altenmüller, M Arenz, M Babutzka, J Barrett, S Bauer, M Beck, A Beglarian, J Behrens, T Bergmann, et al. Improved upper

- limit on the neutrino mass from a direct kinematic method by katrin. *Physical review letters*, 123(22):221802, 2019.
- [36] S Gariazzo, C Giunti, M Laveder, and YF Li. Updated global $3+1$ analysis of short-baseline neutrino oscillations. *Journal of High Energy Physics*, 2017(6):1–38, 2017.
 - [37] M. G. et al. Aartsen. ev-scale sterile neutrino search using eight years of atmospheric muon neutrino data from the icecube neutrino observatory. *Phys. Rev. Lett.*, 125:141801, Sep 2020.
 - [38] P. et al. Adamson. Improved constraints on sterile neutrino mixing from disappearance searches in the minos, MINOS+, daya bay, and bugyey-3 experiments. *Phys. Rev. Lett.*, 125:071801, Aug 2020.
 - [39] AP Serebrov, RM Samoilov, and ME Chaikovskii. Analysis of the result of the neutrino-4 experiment in conjunction with other experiments on the search for sterile neutrinos within the framework of the $3+1$ neutrino model. *arXiv preprint arXiv:2112.14856*, 2021.